Seasonal and Geographical Variation of Blocking

J. SHUKLA

Laboratory for Atmospheric Sciences, NASA/Goddard Space Flight Center, Greenbelt, MD 20771

K. C. MO

M/A-COM Sigma Data, Incorporated, NASA/Goddard Space Flight Center, Greenbelt, MD 20771

(Manuscript received 2 December 1981, in final form 26 October 1982)

ABSTRACT

We have calculated the seasonal variation of frequency of blocking and its geographical location by examining the grid point values of daily 500 mb geopotential height over the Northern Hemisphere for 15 consecutive years (1963–77). Blocking events are objectively identified by requiring that a large positive anomaly of a specified magnitude persist for seven days or more. The magnitude of the threshold anomaly is assumed to be 200 gpm for winter, 100 gpm for summer, and 150 gpm for fall and spring. It is found that the geographical locations of the maximum frequency, characterized by three distinctly different maxima, remain nearly the same in all the four seasons. These maxima which occur in the Pacific to the west of the Rockies, in the Atlantic to the west of the Alps, and over land to the west of the Ural mountains, coincide with the maxima of the low frequency and total variance. If the persistence criterion is changed to 1–3 days, the geographical distribution of frequency for winter is very similar to the 2–6 day band-pass variance, showing maximum values in the areas of storm tracks. Large persistent negative anomalies during the winter season are found to be mostly associated with local high index flow, and in a few instances with a neighboring blocking ridge.

We have also examined the seasonal variability of persistent characteristics of wave numbers 1, 2, 3, 4 for 500 mb geopotential height between 50–70°N. It is found that the large scale planetary waves have preferred phase locations for persistence beyond seven days. It is also found, from the grid point analysis, as well as from the wave number analysis, that seasonal mean anomalies account for less than 25% of blocking events.

1. Introduction

The winter season of the midlatitude atmospheric circulation of the Northern Hemisphere can be mainly described by planetary-scale quasi-stationary features and transient synoptic-scale disturbances in geographically preferred regions. The quasi-stationary patterns are generally considered to be in response to quasi-stationary orographic and thermal forcings associated with mountains, land–sea contrast and zonally asymmetric diabatic heating in the middle latitudes. The synoptic-scale disturbances, i.e., the cyclonic storms off the east coast of North America and Japan, are generally considered to be due to baroclinic instability of the large scale but zonally asymmetric mean flow. The formation, growth, decay and movement of these transient disturbances is of great importance for short-range weather forecasting in midlatitudes, and they have been a topic of comprehensive theoretical, observational and numerical studies during the past 40 years. In addition to the quasi-stationary circulations and transient cyclonic storms, the atmospheric flow pattern is occasionally dominated by quasi-persistent features whose time scale is larger than the life cycle of individual storms, but shorter than the length of a season. The occurrence of such large scale persistent features, generally referred to as blocking, is of great importance for medium range and monthly predictions.

In recent years, there has been a great deal of interest in understanding the possible mechanisms for blocking. Charney and Devore (1979) and Charney and Straus (1980) have suggested that blocking may be one of the multiple equilibrium solutions of a nonlinear system with forcings due to mountains, diabatic heat sources, or both. Charney *et al.* (1981) extended the work of Charney and Devore to incorporate observed zonal topography in a barotropic nonlinear channel model. Within proper range of forcing, two quasi-stable equilibrium states were obtained; one of the stable states resembled the normal winter flow predicted by Charney and Eliassen (1949). Both normal wavenumber 2 and 3 equilibrium patterns have been identified as blocking patterns. Kalnay and Merkine (1981) have suggested that the blocking is the result of nonlinear interaction of Rossby lee waves with stationary forcing. McWilliams (1980) has suggested that even in the absence of any external forcing, blocking may be produced by internal dynamics alone due to balance between nonlinear and dispersive effects.

To the above list of suggested mechanisms, one

must also add the possible role of tropical heat sources. It is being recognized that zonally asymmetric tropical heat sources can be one of the significant forcing mechanisms for midlatitude quasi-stationary circulations (Hoskins and Karoly, 1981), and it is therefore likely that for suitable structures of the zonal flow, fluctuations in the tropical heat sources can also produce anomalies in midlatitude circulation.

In this paper, we have examined the seasonal variation of blocking, where blocking is identified as the occurrence of large persistent anomalies. We hope that an examination of observed variability will give some insight into the possible mechanisms for the occurrence of blocking.

Section 2 of the paper reviews the earlier work on identification and climatology of blocking. Section 3 describes the data used for this study. Section 4 shows the seasonal variability in the location and frequency of blocking events. The locations and frequency of large scale planetary wave anomalies are discussed in Section 5. Finally, conclusions are presented in Section 6.

2. Review of earlier work

The first systematic empirical and semi-statistical study of blocking activity in the Northern Hemisphere westerlies was reported by Elliott and Smith (1949). They examined 40 years of daily pressure values for January and February from the Historical Weather Map Series (U.S. Weather Bureau). The basic data consisted of grid point values (5° latitude × 10° longitude) in the region 35–60°N and the 140–40°E quadrant. They examined the blocking activity in three different regions: Pacific (140°E–135°W), North America (130–60°W), and Atlantic (55°W–40°E). They used an objective criteria based on magnitude and persistence of pressure departure from normal. Following these criteria, which were different for Pacific and Atlantic, they determined the exact dates of inception and duration of blocking events which were first identified and catalogued subjectively.

According to the definition of blocking action by Elliott and Smith (1949), the number of mid-Pacific blocking events was twice as many as in the northeastern Atlantic, and the total number of blocking days for the mid-Pacific were four times as many as in the northeastern Atlantic. It should be remarked that this difference in frequency of blocking events in the Pacific and the Atlantic could be, at least in part, due to differences in the criteria for identifying the blocking events. Elliott and Smith (1949) also examined the interannual variability of blocking action and its relation to sun spot cycles.

Rex (1950a,b) examined the Northern Hemisphere daily 500 mb flow patterns and 3-km and surface charts for 19 years (1932–50) to determine a catalogue of blocking events. He first identified the blocking events subjectively by visual inspection and then used semi-objective criteria to determine the exact dates of initiation and duration of blocking.

Rex showed that the occurrence of blocking has two preferred locations, the Atlantic blocking, 60°W–20°E, and the Pacific blocking, 180–120°W. There were 82 occurrences of the Atlantic blocking and 30 of the Pacific blocking. He calculated the percentage of blocking days for each month and showed that for both the Pacific and the Atlantic, the maximum occurs in April–May (23% for Pacific and 40% for Atlantic), and the minimum occurs in August–September. For the Pacific, the summer minimum was zero and for Atlantic, the summer minimum was ~15%. He also calculated the frequency of blocking as a function of duration of persistence in days and showed that the maximum frequency occurred for 14 days. The average duration for all the cases was 16.6 days. It should be noted that his statistics of frequency and persistence were calculated only for those events which were first catagorized as blocking and, therefore, frequency was not calculated for those events which persisted for less than 10 days.

It is interesting to note that the papers by Elliott and Smith (1949) and Rex (1950a,b), which were published within a year, gave contradictory results on the relative frequency of blocking in Atlantic and Pacific. Elliot and Smith showed that blocking was more frequent in Pacific, whereas Rex showed it to be more frequent in Atlantic. Their synoptic criteria for identifying the blocking events were different as well as the criteria for duration of days. This points to a basic problem in identifying and cataloging blocking events. Many questions arise: Should one examine surface maps or upper air maps? Are time averaged (weekly or monthly) maps more suitable than daily maps? What is the most appropriate meteorological parameter for which variability should be examined? Should the criteria for choosing a blocking event be subjective or objective? What should be the minimum duration of persistence before an event can be categorized as blocking? Should one examine the total flow field or only its departure from a climatological mean state? etc.

While most of these questions still remain unanswered, there are several other papers following Elliott and Smith, and Rex, who have examined the occurrences of blocking phenomena. Brezowsky *et al.* (1951) categorized the blocking highs by examining the anticyclonic axis over the northeastern Atlantic and northern Europe for a 70-year period (1881–1950). They found that, in agreement with the results of Rex, the frequency of blocking was maximum in May and minimum during July and August. Sumner (1954) used a purely subjective approach to categorize the blocking events and studied their geographical

and seasonal distribution in the Atlantic–European sector of the Northern Hemisphere. He did not demand persistence as a criterion to define blocking. Sumner found that the blocking is most frequent in May and least frequent in July, with a secondary maximum in November.

White and Clark (1975) examined the Northern Hemisphere monthly mean maps of sea level pressure and 700 mb geopotential height for the period (1950–70). They concluded that the frequency of blocking over the north Pacific is a maximum during the autumn and winter seasons (October–March) and minimum during spring and summer. The maximum value of frequency occurred in January. This result was not in agreement with Rex (1950b) who had found that the blocking action has maximum frequency in spring (April and May) and minimum frequency in late summer (August and September). White and Clark concluded that this discrepancy occurred because Rex included the blocking activity over the Rocky Mountains, which they found to be primarily a spring–summer phenomenon.

A day-to-day Fourier analysis was made of 500 mb heights and the sea level pressure using data from U.S. Daily Synoptic Weather maps from 1966 to 1976 by Austin (1980). She suggested that the wavenumber 1 to 4 were crucial in initiating and destroying the blocking.

Dole (1978) suggested a truly objective technique, such that 500 geopotential height, or any other data could be machine-processed, to identify blocking events. According to Dole, "blocking exists whenever a positive 500 mb geopotential height departure from the climatological mean height of one standard deviation or greater persists over at least one grid point for a period of at least ten days." Persistence criterion of 10 days and anomaly magnitude of 100 gpm were chosen arbitrarily.

Based on above criteria, Dole (1982) calculated the frequencies of persistent anomalies by using 14 years of winter 500 mb heights data. He found three major favored regions for the occurrence of persistent anomalies: the North Pacific, the North Atlantic and the north Soviet Union. For each region the maximum in the frequency of occurrence of positive anomalies and negative anomalies coexisted, and had comparable magnitudes.

Charney *et al.* (1981, hereafter referred to as CSM) followed Dole's method, but analyzed the past data to find a natural basis for determining the threshold criteria of persistence. They examined the product of frequency and days, with respect to duration of persistence, and found that a clear maximum occurs for two days and a significant discontinuity occurs near seven days. This led them to conclude that the day-to-day fluctuations of the atmosphere are characterized by two distinct processes, one due to baroclinically unstable synoptic-scale disturbances, for which the geopotential anomaly persists for 1–3 days, and the other due to the occurrence of blocking events, for which the geopotential anomaly persists for seven days or more.

CSM did not test the significance of the second discontinuity near seven days. We have subsequently made similar calculations for a first order autoregressive time series with reasonable choices of autocorrelation at lag 1. (See Appendix). We have generated large numbers of time series and carried out the same analysis as CSM. It is found that a discontinuity occurs only for large persistence period or small sample size. This suggests that the discontinuity near seven days found by CSM might be a consequence of physical processes different from synoptic scale instabilities. We have also shown in this paper that the maximum near two days corresponds to storm tracks in the midlatitudes.

Since the atmospheric fluctuations can be considered as comprised of a linear combination of a spectrum of space and time scales, it should be determined whether a linear superposition of different space and time scales can produce large, regional anomalies. We have generated a large number of time series with realistic space–time spectra and again we have found no evidence of a discontinuity as found in the observations.

This brief review of the earlier works points to a difficulty in defining and identifying blocking events from observed data. The choice of criteria, the shape of the pattern, and the duration of persistence can give different distributions in space and time. Here, for the purpose of studying the seasonal variability, we have followed the approach of adopting objective criteria as originally suggested by Elliott and Smith, and later by Dole, and examined the geographical locations and frequency of large scale persistent anomalies.

3. Data

The data used in this study are twice-daily 500 mb geopotential height fields for 15 years from 1 January 1963 through 31 December 1977, over the Northern Hemisphere between 20 and 90°N. The data are the NMC analyses which we obtained from Mr. Roy Jenne of NCAR[1]. This data set, as received from NCAR, contained several missing days and several unrealistic values for 500 mb geopotential height. Day to day changes, and spatial and temporal consistency were checked for the entire 15 year period. Missing and doubtful dates were filled in by linear extrapolation from adjacent dates.

Geopotential height ϕ at any grid point, is ex-

[1] NCAR is the National Center for Atmospheric Research and is sponsored by the National Science Foundation.

pressed as

$$\phi(t) = \bar{\phi} + \sum_{n=1}^{N} A_n \cos\omega_n t + B_n \sin\omega_n t,$$

where $\bar{\phi}$ is the 15 year mean, A_n, B_n are Fourier coefficients for frequencies ω_n, $n = 1$ corresponds to a period of 15 years, and $n = N = 5475$ ($=365 \times 15$) corresponds to a period of one day. The seasonal cycle ϕ_s is defined as the sum of annual (ω_{15}) and semiannual (ω_{30}) components and the 15 year mean, i.e.,

$$\phi_s(t) = \bar{\phi} + A_{15} \cos\omega_{15} t + B_{15} \sin\omega_{15} t + A_{30} \cos\omega_{30} t + B_{30} \sin\omega_{30} t.$$

The anomaly ϕ' at a grid point is defined as

$$\phi'(t) = \phi(t) - \phi_s(t).$$

We have calculated the daily values of ϕ' at each grid point (4° latitude × 5° longitude) between 20 and 90°N for 15 years. The winter season consists of December, January and February; spring consists of March, April and May; summer consists of June, July and August; and fall consists of September, October and November.

4. Locations and frequency of blocking event

We calculate the blocking frequency at each grid point for four seasons separately. If ϕ' of a given magnitude ($\geq +200$ gpm for winter, $\geq +150$ gpm for fall and spring, and $\geq +100$ gpm for summer) persists for seven days or more, we count the whole period as one blocking event. These threshold values of persistence were determined by examination of past data and as described by CSM. There appears to be a physical basis for distinguishing between storm tracks (persistence for 1–3 days) and large-scale persistent anomalies. We recognize that the occurrence of a positive anomaly does not necessarily mean the existence of a blocking ridge, because a weaker climatological trough will also give a positive ϕ'; however, for the purpose of this simple analysis of seasonal variability, we use this definition uniformly for all the four seasons. Once the above criteria are prescribed, the rest of the calculations and the results are produced objectively.

Figs. 1a, b, c and d show the standard deviation of daily values for 15 winter, spring, summer and fall for 500 mb geopotential heights, respectively. These maps are very similar to those presented by Blackmon (1976) using 10 years of data. The largest contour value on the map for winter is 200 gpm which is chosen as the threshold value for ϕ' to persist for seven days or more. Examination of standard deviation for the other three seasons suggests a threshold value of 100 gpm for summer and 150 gpm for fall and spring.

Figs. 2a, b, c and d show the maps of frequency of occurrence of persistent anomalies for the four different seasons, winter, spring, summer and fall, respectively. It is seen that all four maps show three different maxima and these maxima occur generally in the same area. A small exception occurs for the maximum near Greenland, which is displaced northeastwards during summer and fall. The maxima in the Pacific and Atlantic were identified by Elliott and Smith (1949), and Rex (1950) in their earlier work. A third maximum near the Ural Mountain ranges of USSR is found to be rather prominent in the summer season also. It should be noted that different threshold values for anomaly magnitude have been used to define blocking in different seasons and that the frequency values for different seasons have about the same magnitude. If we calculate the number of events using the same criteria (positive anomalies of 100 gpm or more persist for seven days or more) for all four seasons, then the number of persistent events is higher in winter and fall, and lower in spring and summer.

In the following section, we have analysed the winter season data in more detail to examine the persistence characteristics of large negative anomalies, and geographical distribution of large positive anomalies which persist only for 1–3 days.

It should also be recalled that to define the anomaly ϕ' we removed only the 15-year mean, and annual and semiannual periods from observed values. It is likely that some of the events shown in Fig. 2 could be simply due to an anomalous seasonal mean. We have recalculated the frequency map for the winter season after removing the seasonal mean for each year separately, and the result is shown in Fig. 3. Comparison between Figs. 2a and 3 show that the locations of maxima are the same in both maps but the frequency values have been reduced by ~25%.

The fifteen-year data set was split into an eight-year period (1963–70) and a seven-year period (1971–77), and the frequency of occurrence of persistent anomalies for winter season was calculated separately for each period. It was found that the locations of the maximum frequency remained the same in both the data sets and the number of events were comparable in both periods.

a. Persistent negative anomalies

CSM (1981) have shown that large persistent negative anomalies are less frequent compared to large persistent positive anomalies. Large positive anomalies which persisted for seven days or more were identified as blocking events and appeared in association with an amplified blocking ridge. The persistent large negative anomalies, however, were associated with local high-index flow. If the long term mean flow pattern has a climatological ridge in a given area, and if we define the anomaly as a departure from this climatological mean, an "abnormal" zonal flow configuration will be identified as a large

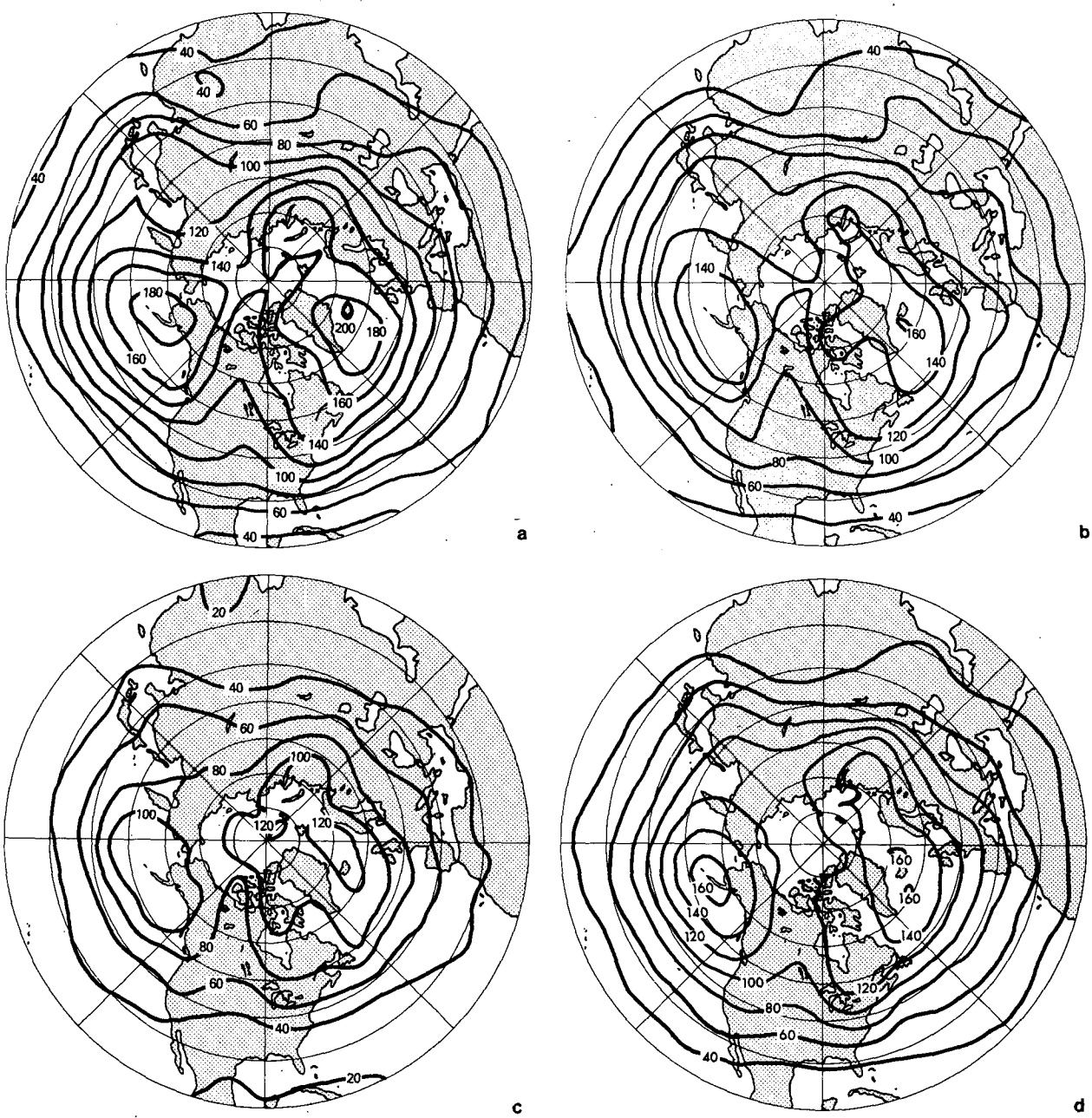

FIG. 1. The standard deviations of daily values of 500 mb heights for (a) winter, (b) spring, (c) summer, (d) fall. Contour interval is 20 m.

negative anomaly. This points to the limitations of examining anomalies rather than total flow and the possible misinterpretation of large negative anomalies as deep troughs can be avoided by examining the total field.

Fig. 4 shows a frequency map calculated from 15 winter seasons for negative anomalies of −200 gpm or less. The persistence criterion is still seven days or more. This map also shows three different maxima; however, the frequency values are smaller. If the cut-off magnitude is chosen as −100 gpm instead of −200 gpm then the frequency value of occurrence of persistent negative anomalies is comparable with the frequency value of persistent positive anomalies as shown by Dole (1982). It should be pointed out, however, that the maxima for the negative anomalies are displaced southeastward compared to the maxima for the positive anomalies for the Atlantic and Pacific. Comparison between Figs. 2a and 4 suggests, as found by CSM, that large negative anomalies are not as frequent as large positive anomalies.

Our winter season results are generally in good

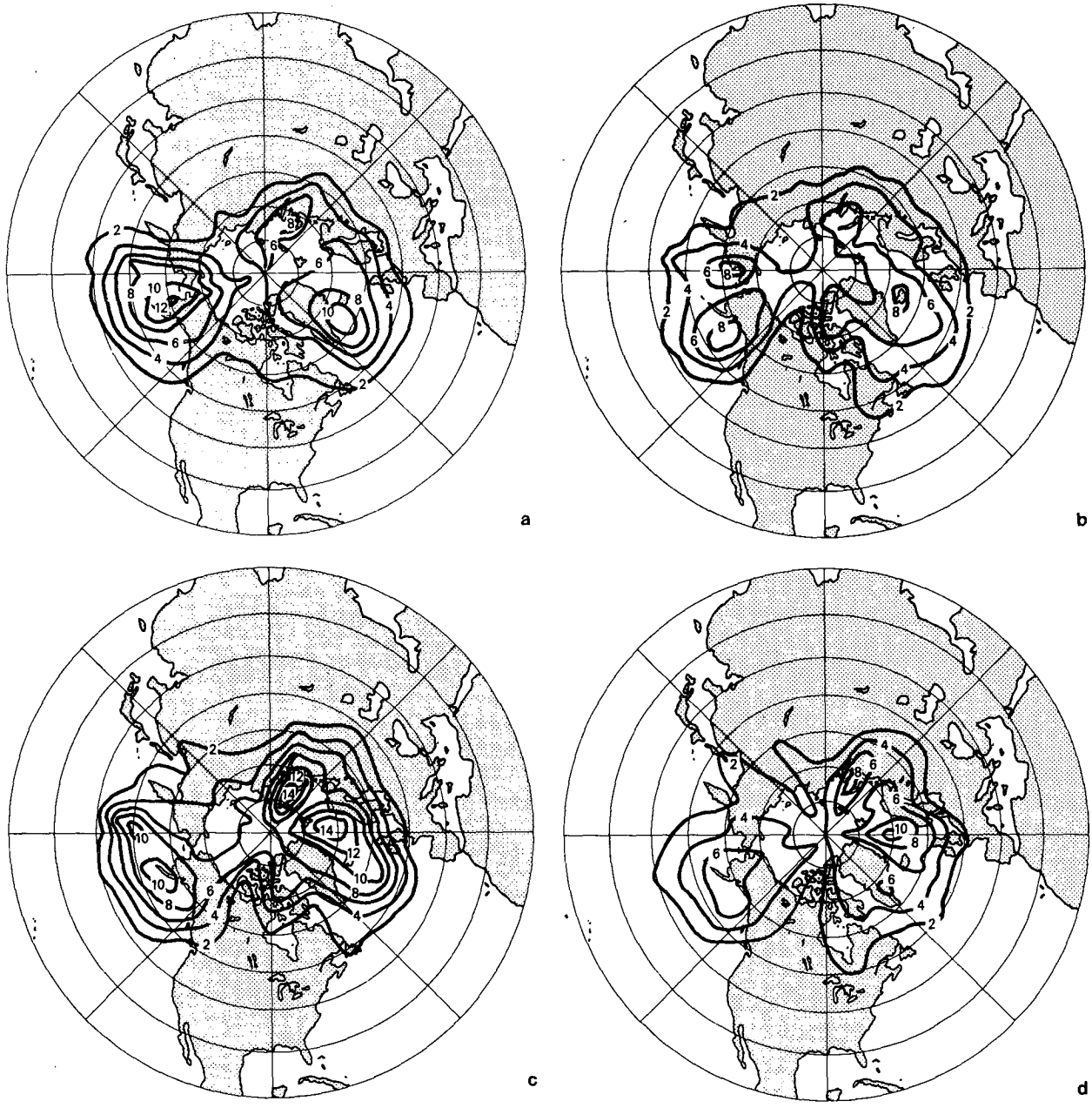

FIG. 2. Number of events per 15 years of 500 mb height positive anomalies: (a) 200 gpm or more persist for seven days or more during winter; (b) 150 gpm or more persist for seven days or more during spring; (c) 100 gpm or more persist for seven days or more during summer; (d) 150 gpm or more persist for seven days or more during fall. Contour interval is 2.

agreement with Dole's. However, the locations of maximum frequency are shifted equatorward in Dole's results because he has normalized the geopotential anomalies by the Coriolis parameter. We found that the magnitude of frequency of occurrence for positive and negative anomalies is comparable only for the criteria chosen by Dole, and for magnitude criteria of ±200 gpm as chosen by us, the frequency of events for negative anomalies is considerably less compared to positive anomalies. We also found that large persistent negative anomalies are associated with high-index flows.

We have separately averaged all the events that contributed to the maximum frequency of negative as well as positive anomalies at 62°N, 20°W and surrounding nine grid points. The actual dates for the occurrence of these negative anomaly events are: 6–13 December 1964; 10–18 January 1965; 16–22 February 1967; 19–25 January 1971; 18–26 January 1972; 1–8 December 1972; 3–16 January 1974; 9–15

February 1974; 25–31 January 1974; 22–31 January 1975; 1–8 December 1976. Fig. 5a shows the mean of these eleven events, and it is seen that these events of large persistent negative anomaly were associated with local high-index flow. Fig. 5b shows a similar composite of all five events (23–31 December 1963; 20–29 February 1968; 13–22 February 1970; 16–24 January 1973; 18–27 February 1975) that contributed to the maximum frequency at 50°N, 160°W, and nine surrounding grid points. It is seen that the mean flow in the region is high-index type. The remaining three events (17–24 December 1969; 7–15 February 1972; 2–22 February 1977) of large negative anomaly at 50°N, 160°W occurred in conjunction with an upstream blocking ridge. These results show that for the 15-year winter data examined here, most of the events of large persistent negative anomaly (in the region of maximum frequency in Fig. 4) were associated with local high-index flow.

Fig. 5c shows a similar mean of these positive events (8 January–4 February, 1963; 24 January–10 February 1965; 14–28 February 1965; 2–12 January 1967; 8–18 February 1968; and 21 December–7 January 1971) that contributed to the maximum frequency at 62°N, 20°W. Fig. 5d shows mean of positive events (6–30 January 1963; 1–7 December 1966; 17 December–6 January 1965; 18–27 February 1972; 2–12 December 1972; 1–10 January 1971; 2–11 January 1973; 1–10 January 1974 and 27 January–12 February 1975) which contributed to the maximum frequency at 50°N, 160°W. Contrary to the composites of negative anomaly events, where there is no evidence of an enhanced trough, we can see clearly that the positive anomaly events show an enhanced blocking ridge at the designated place.

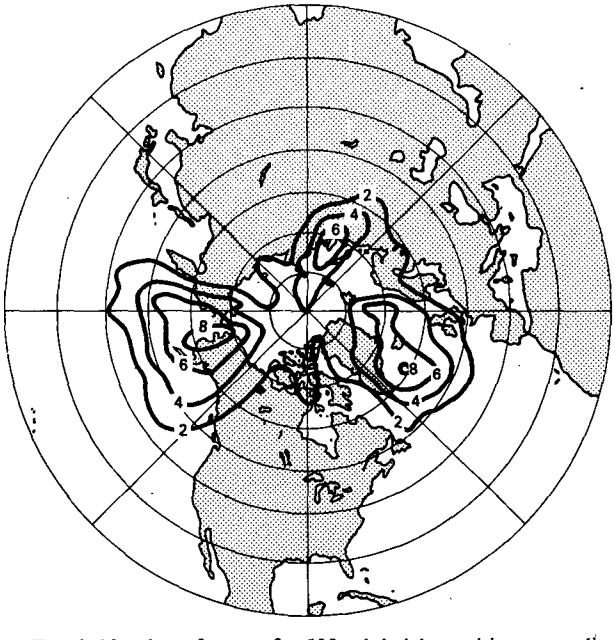

FIG. 3. Number of events for 500 mb height positive anomalies of 200 gpm or more persist for seven days or more during winter when the 90 day mean of each individual winter is subtracted from the anomaly; contour interval 2.

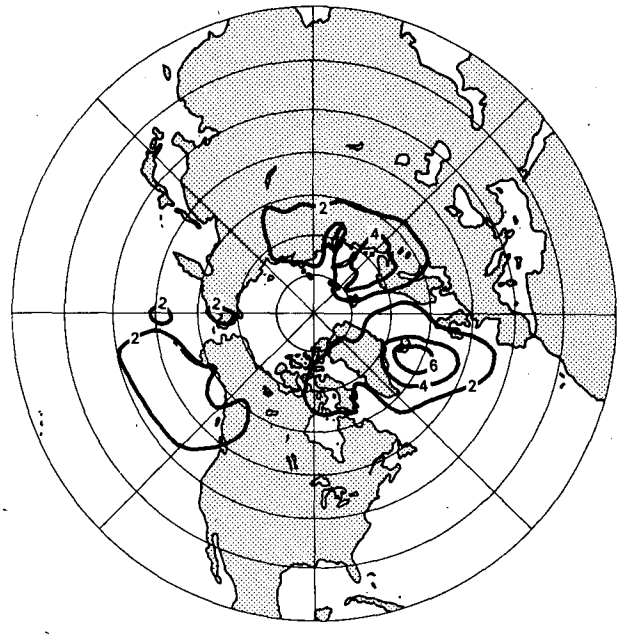

FIG. 4. Number of events for 500 mb height negative anomalies of −200 gpm or less persist for seven days or more during winter; contour interval 2.

b. Composite structure of blocking

To study the large scale structure of blocking events, composite maps were made for each sector: Pacific (ridges between 170°E and 165°W), Atlantic (ridges between 10°E and 30°W), and Russian (ridges between 60 and 45°E), for all four seasons. For the winter season, the dates of all blocking events are listed in CSM. Here we show composite maps of Pacific, Atlantic and Russian sector blocking events during the winter season only. The composite map was prepared with respect to the location of the ridge along the longitude of maximum positive anomaly.

There were 15 blocking events in the Pacific sector and all maps were rotated such that blocking ridge falls along 180°. Similarly, there were 20 cases in the Atlantic sector with ridges lined up along 20°W, and six cases in Russian sector with ridges lined up along 45°E.

Fig. 6a–6c show the composite maps for Pacific, Atlantic and Russian sectors, respectively. The composite structures of blocking have the same basic features for all three centers and they change very little from season to season. A negative anomaly occurs to the south of the large positive anomaly. A negative anomaly also occurs to the east and west of the large positive anomaly at a distance of ~45–60° of lon-

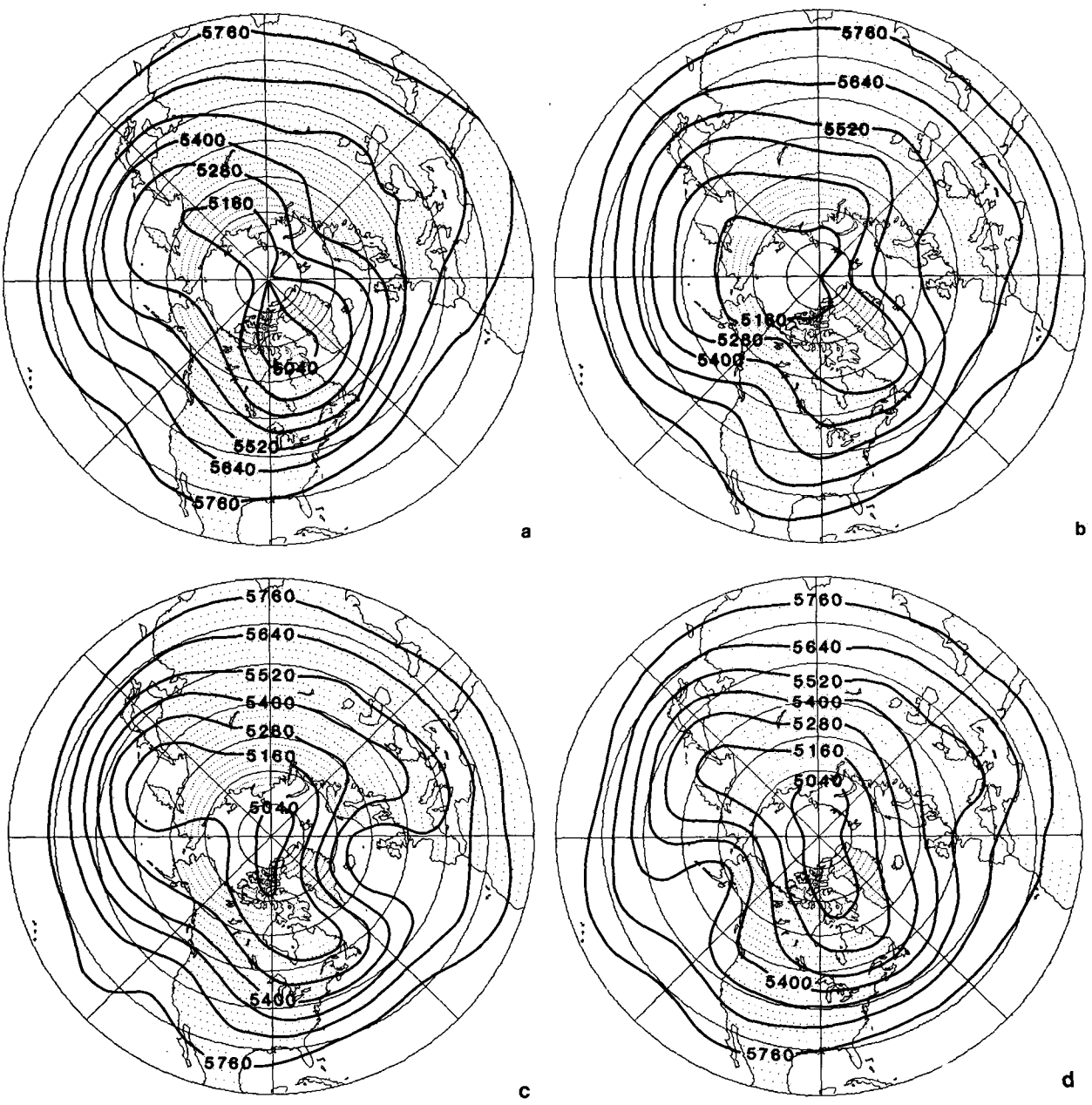

FIG. 5. Mean of (a) 11 events which contribute to the maximum frequency of negative anomalies at 62°N, 20°W; (b) 5 events which contribute to the maximum frequency of negative anomalies at 50°N, 160°W; (c) 6 events which contribute to the maximum frequency of positive anomalies at 62°N, 20°W; (d) 9 events which contribute to the maximum, frequency of positive anomalies at 50°N, 160°W. The contour interval is 120 m.

gitude. The negative anomaly just south of the large positive anomaly is strong in Pacific and Atlantic sectors, and very weak in the Russian sector. The negative anomaly downstream of the blocking ridge is generally stronger than the upstream negative anomaly. The composite map for the Russian sector shows a very strong wavenumber 3 pattern in all seasons except in the summer.

c. Persistence for 1–3 days and storm tracks

It was suggested by CSM that persistent anomalies for 1–3 days represent baroclinically unstable synoptic-scale disturbances. We have calculated frequency maps for anomalies of 200 gpm or more and persistence of 1–3 days for all four seasons. The frequency map for the winter season (Fig. 7) looks very

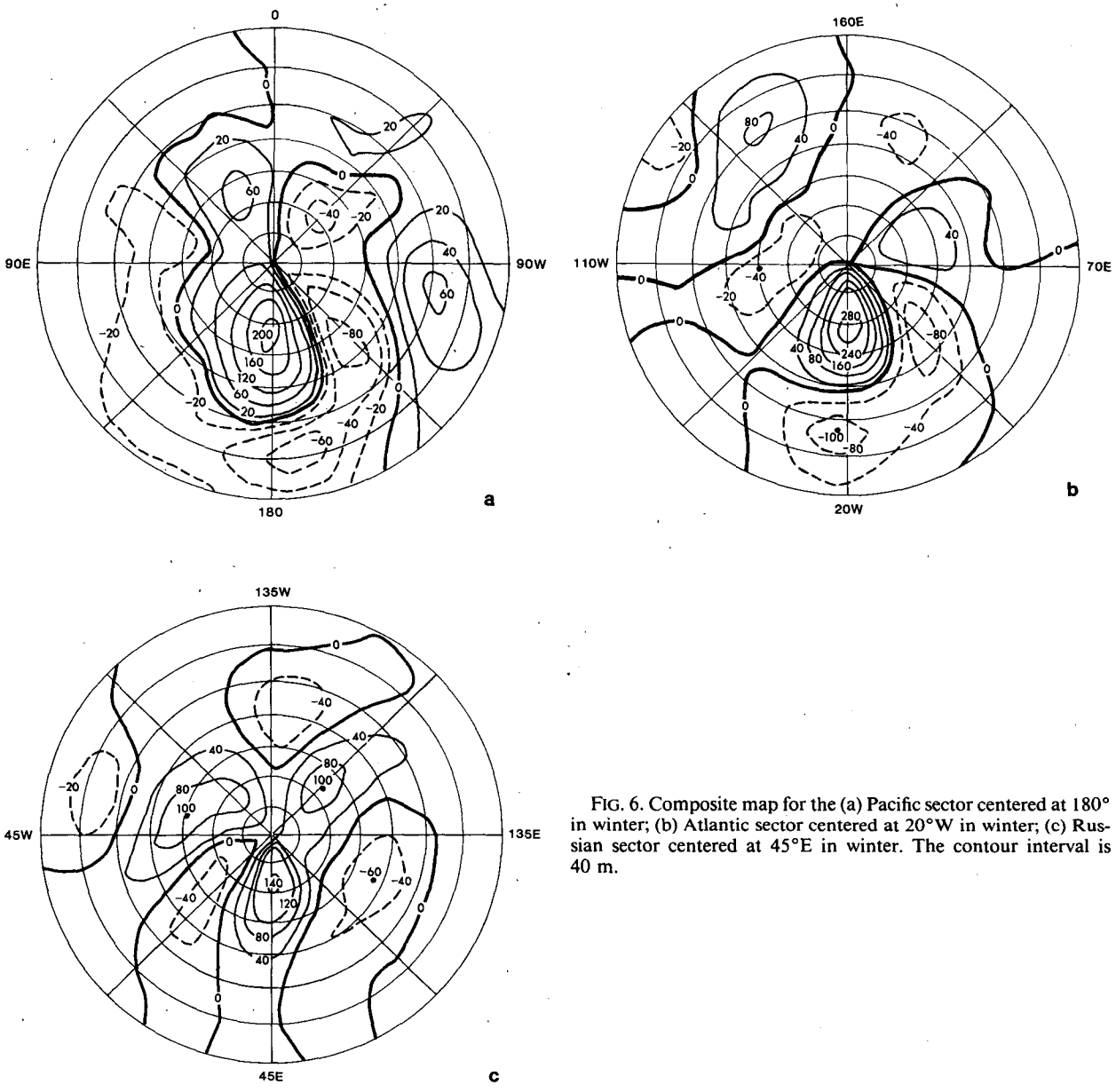

FIG. 6. Composite map for the (a) Pacific sector centered at 180° in winter; (b) Atlantic sector centered at 20°W in winter; (c) Russian sector centered at 45°E in winter. The contour interval is 40 m.

similar to the map of 2–6 day band-pass variance shown by Blackmon (1976), which supports the contention that 1–3 day persistent anomalies represent storm tracks. Similarity between 1–3 day persistence-frequency map and band-pass variance is equally good for the other three seasons (not shown). During summer, there is no marked difference between the locations of maximum frequency for 1–3 days persistence and more than seven days persistence which is in agreement with Blackmon (1976), who showed that there is no marked difference in geographical locations of total low-pass and band-pass variance during summer.

5. Persistence of large scale planetary wave anomalies

At each latitude J and time t, the anomaly field at longitudes (I) can be decomposed into zonal waves

$$\phi'(J, I, t) = \phi'_0(J, t) + \sum_k \phi'_k(J, I, t),$$

$$\phi'_k(J, I, t) = A_k(J, t) \cos(2\pi kI/\mathrm{Im}) + B_k(J, t) \sin(\pi kI/\mathrm{Im},$$

where Im = 72 is the number of grid points at a given latitude. A_k, B_k are Fourier coefficients of wavenumber k.

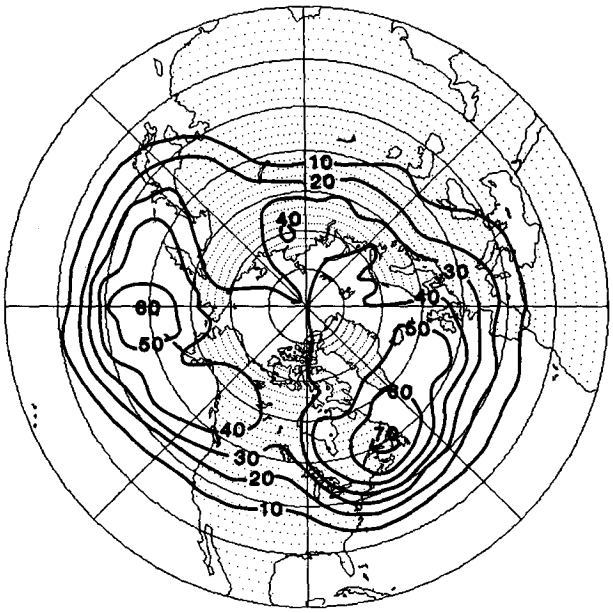

FIG. 7. Number of events for which positive anomalies of 200 gpm or more persist for 1–3 days during winter; contour interval 10.

For each wavenumber we reconstruct the geopotential anomaly field at all grid points ϕ'_k and we examine ϕ'_k separately for each wave number to calculate the frequency of persistent positive anomalies at each grid point for four seasons separately. When ϕ'_k of a given magnitude (60 gpm for k = 1, and 2, 40 gpm for k = 3, and 20 gpm for k = 4) or more persists for seven days or more, it is counted as one event. Then we sum up all frequencies between 50–70°N. The solid line in Figs. 8 and 9 shows the frequency of occurrence of positive anomalies for wavenumber 1 or 2 where ϕ'_k satisfies the above criteria. The dashed line shows the frequency of occurrence when the 90 day mean of individual year was removed before calculating ϕ'_k. Figs. 10 and 11 show the frequency of occurrence of positive anomalies for wavenumber 3 and 4 respectively. The normal winter mean positions for the wavenumber 3 ridge is near 100°E with an amplitude of 47 gpm, and for the wavenumber 4 ridge it is near 160°E with an amplitude of ~17 gpm.

There are two distinct maxima at 55°W and 145°E for wavenumber 1. With the 90 day mean removed, the frequency generally has the same shape with the maxima shifted to 60°W and 130°E, and there is an additional maximum at 30°W. The amplitude of the 15-year winter mean wave number 1 is 60 gpm and has a ridge at 5°E. By examining the synoptic maps of total ϕ-field, we conclude that there are two preferred locations for persistent ridges of wavenumber 1 field. Furthermore, Fourier analysis of the anomaly field of all 35 blocking events in winter listed in CSM shows that for blocking events where the amplitude of wavenumber 1 is larger than 60 gpm, these are two favored ridge positions. Since these two ridges are not close to the climatological mean, the blocking is not due to the resonance between stationary wavenumber 1 and transient wavenumber 1. The two ridges are 180° apart which suggests their possible association

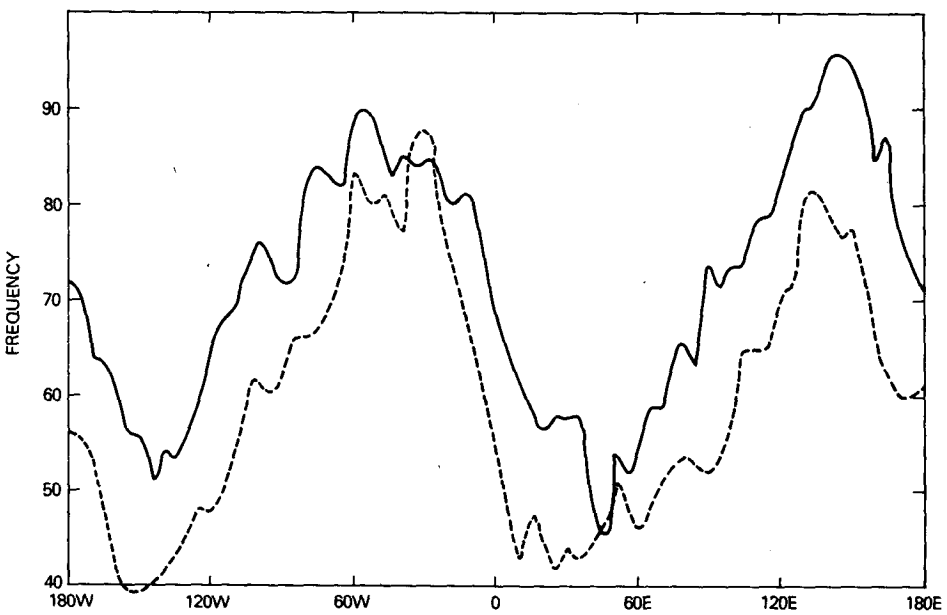

FIG. 8. Number of events for which positive anomalies of 60 gpm or more persist for seven days or more for wavenumber 1 during winter.

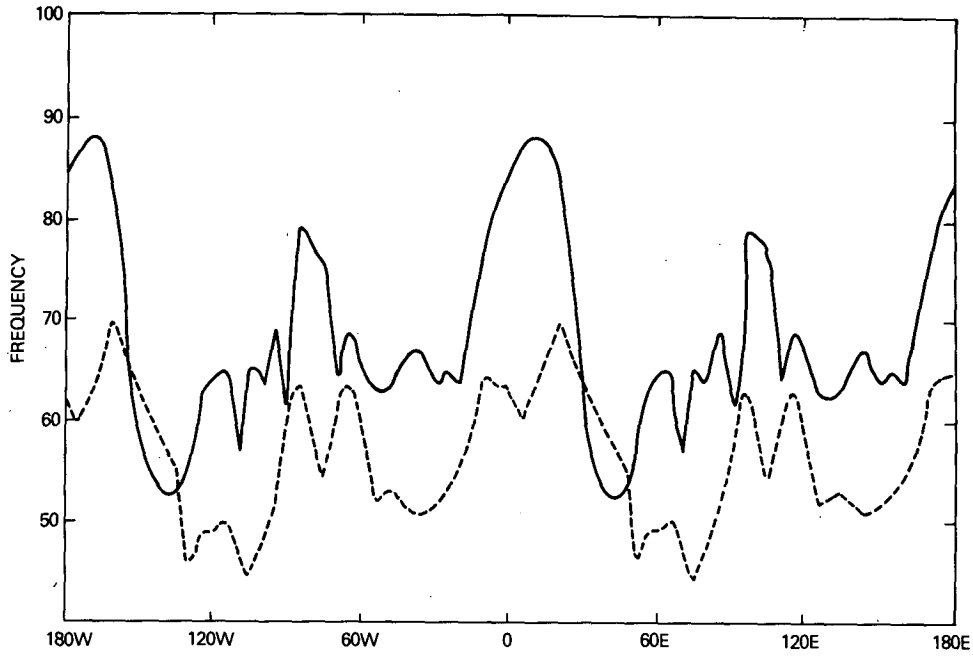

FIG. 9. As in Fig. 8, but for wavenumber 2 during winter.

with subresonant and superresonant response to orographic forcing.

There are four maxima for wavenumber 2. Two strong ones at 170°W and 10°E, and two weaker ones at 85°W and 95°E. If the 90 day mean is removed, the frequency maxima are not as strong, but they remain at the same locations. The amplitude of 15-year mean wavenumber 2 is 76 gpm and the ridge occurs at 55°E and 125°W. The four maxima shown here are preferred locations for persistent ridges of wave number 2 anomaly field. It should be noted that CSM used a simple barotropic nonlinear channel model with observed zonal topography and predicted two equilibria associated with wavenumber 2 resonance. The superresonant wavenumber 2 solution had ridges at 110°W and 80°E; the subresonant solution had ridges at 160°W and 10°E. The predicted ridge positions are in reasonable agreement with the observations.

The frequency curve for wavenumber 3 has three maxima at 85°W, 35°E and 155°E and three secondary maxima at 135°W, 15°W and 105°E.

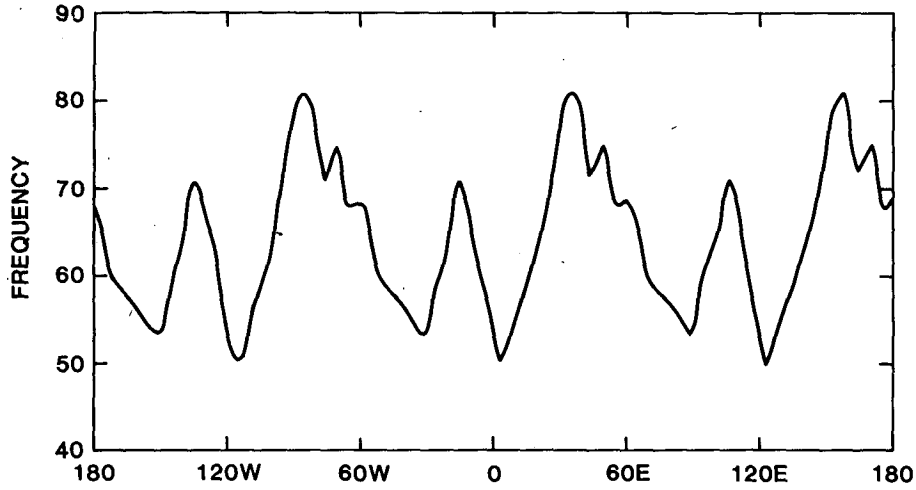

FIG. 10. As in Fig. 8, but for positive anomalies of 40 gpm or more for wavenumber 3 during winter.

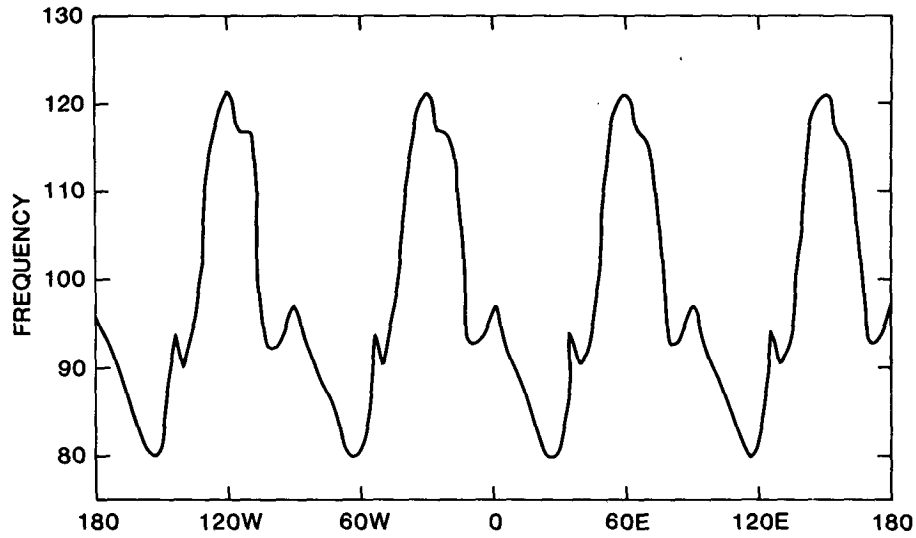

FIG. 11. As in Fig. 8, but for positive anomalies of 20 gpm or more for wavenumber 4 during winter.

The frequency curve for wavenumber 4 shows four maxima which coincide with the normal ridge positions for the winter mean.

Figs. 12 and 13 show the seasonal variation of frequency of occurrence of large persistent anomalies of ϕ'_k corresponding to wave numbers 1 and 2. The frequency values for summer and fall are small, and there are no significant maxima. For spring, the frequency has a maximum at 70°W and a much weaker one at 170°E for wavenumber 1. The maxima for

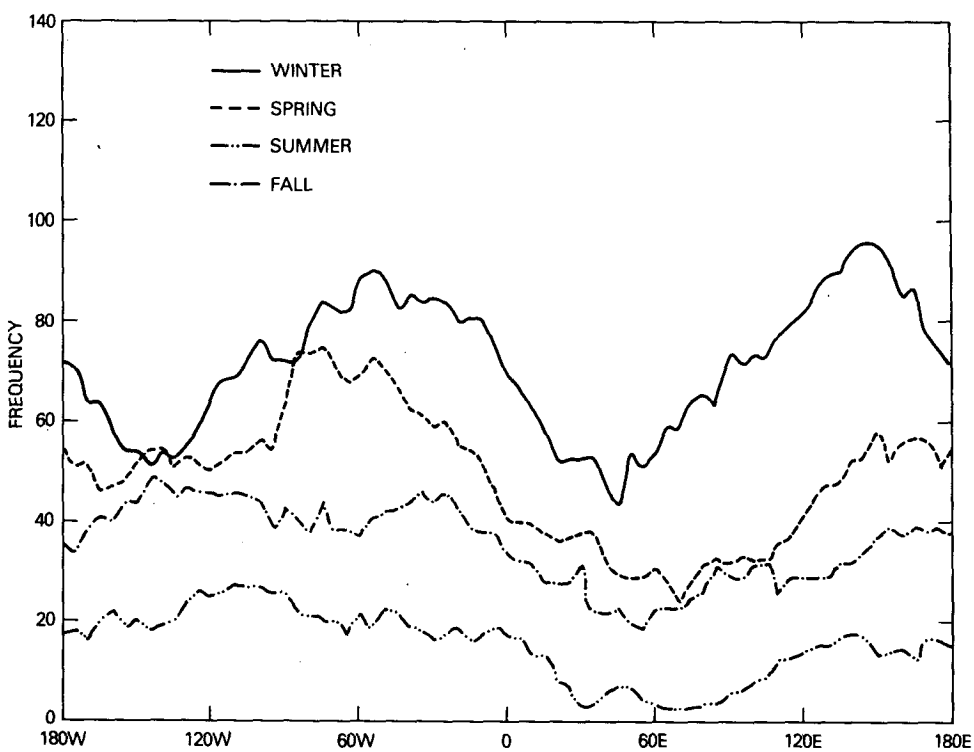

FIG. 12. Seasonal variation of frequency for wavenumber 1.

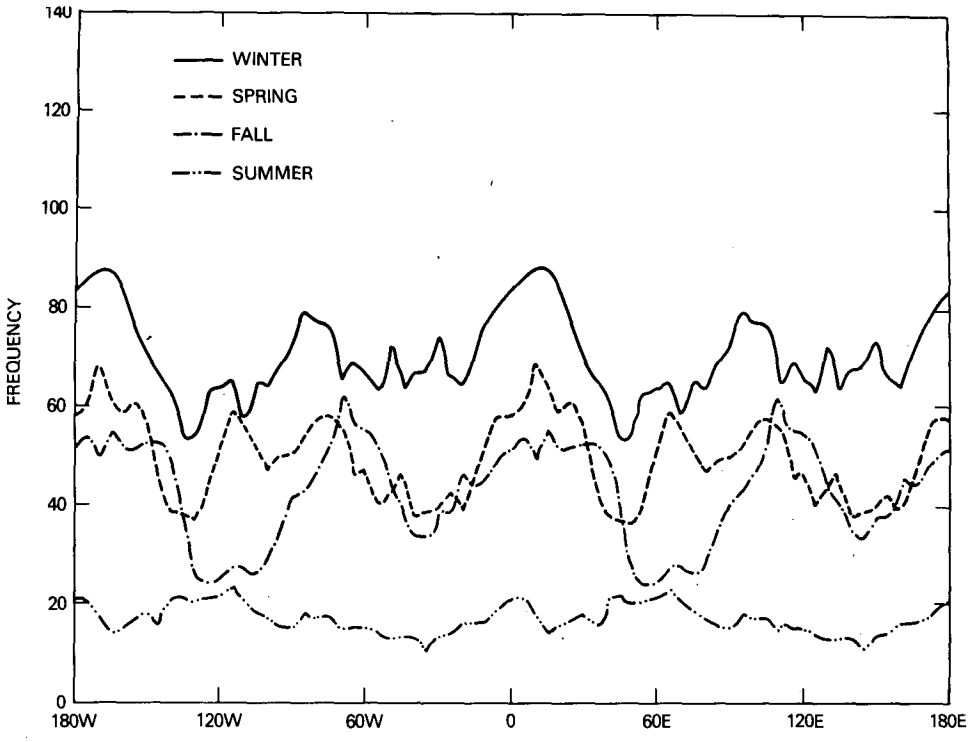

FIG. 13. As in Fig. 12, for wavenumber 2.

spring are 170°W, 10°E, 65°W, and at 115°E for wavenumber 2. The seasonal variations of frequency are not significant.

6. Conclusions

1) Large scale persistent anomalies of positive sign are more frequent than those of negative sign. As also noted by Charney *et al.* (1981), amplified blocking ridges persist longer than either deep troughs or weaker ridges.

2) There are three distinct centers of maximum blocking activity. They occur in the Pacific to the west of the Rockies, in the Atlantic to the west of the Alps and Scandanavian Mountain ranges, and over land to the west of Ural Mountains. The local structure of blocking in all three regions is very similar. *These relatively preferred locations of persistent anomalies and their local structures do not change with season.*

3) A persistence criterion of 1–3 days represents storm track patterns, and the resulting features are distinctly different from the persistence criterion of seven days or more.

4) The maxima of frequency of occurrence of large positive and negative persistence anomalies occur in the same region. The large persistent negative anomalies are mostly associated with abnormal straight zonal flows.

5) Occurrence of anomalous seasonal mean anomalies accounts for less than 25% of the persistent anomalies identified as blocking events.

6) The large anomalies of planetary waves also have preferred regions of persistence. In general, they are associated with blocking events.

Acknowledgments. This work is an outgrowth of our earlier study on the observational evidence of multiple equilibrium states in the atmosphere which was conducted in collaboration with Professor J. G. Charney. An attempt to understand the mechanisms of blocking lead us to examine the nature of seasonal variability of blocking. We are especially grateful to Mr. B. Doty and Mr. D. Gutzler for their help in preparing a 15-year continuous time series of geopotential fields. Mr. Gutzler gave valuable suggestions during the study. We are grateful to Professor R. S. Lindzen for conducting a series of seminars on blocking and providing continuous stimulation for this project. In particular, Professor Lindzen suggested to examine the role of seasonal mean anomalies in determining the intensity of individual blocking events. We thank Dr. D. Straus for providing us the space–time spectra of observations. We would also like to thank Professor Kevin E. Trenberth for many valuable suggestions on the earlier manuscript.

We thank Mrs. J. Reckley for typing the paper and Mrs. L. Rumburg for drafting the figures.

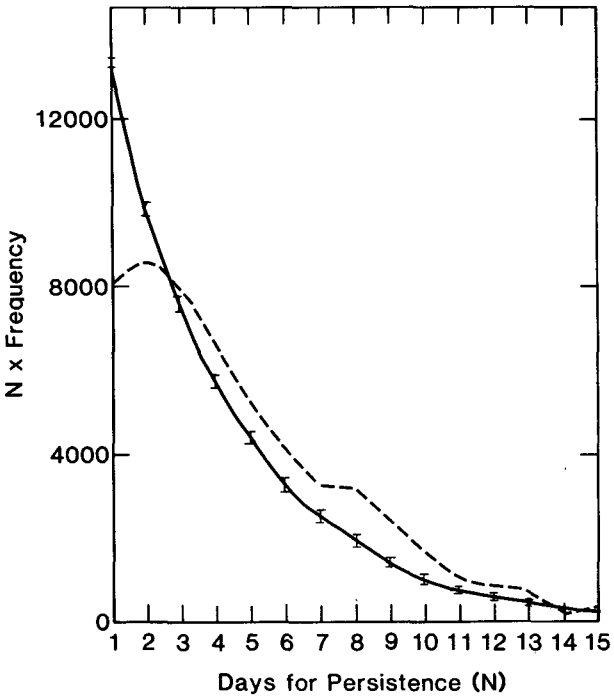

FIG. 14. Frequency × duration versus duration averaged for 50 different realizations of Markov time series (solid line). The error bars are standard deviations among 50 realizations. The dashed curve is reproduced from Charney *et al.* (1981).

APPENDIX

Persistence characteristics

a. First order Markov time series

CSM (1981) calculated the frequency of occurrence of persistent anomalies for 360 grid points (50–70°N) over the Northern Hemisphere using daily 500 mb geopotential height data for 15 winter seasons. Thus, they had 474 840 data samples (all not independent samples because of spatial and temporal correlations of geopotential height field), 10% of which had magnitudes ≥200 gpm which were used for their Fig. 8. We have generated a first-order Markov time series with 1400 samples at 432 grid points and combined 604 800 data samples to calculate a curve similar to CSM.

The discrete time series Y_n is given as

$$Y_n = RY_{n-1} + X_n \quad (\text{for } Y_0 = 0),$$

where R is the autocorrelation at lag 1; X_n is a normally distributed random time series with a mean of 0 and a standard deviation of 1.

It should be noted that Y_n is also normally distributed with zero mean and standard deviation of $(1 - R^2)^{-1}$. The only parameter to be specified is the value of R. We have calculated the actual values of R at 432 grid points (50–70°N, at 4° interval) over the Northern Hemisphere from observed daily 500 geopotential height for 15 (1963–77) winter seasons. Values of R range between 0.61 and 0.88 with most of the values within the range of 0.7–0.8. We have used these values of R to generate the time series Y_n at each grid point separately. We have generated 50 separate realizations of such time series and calculated the frequency of persistence when $Y_n \geq 2.25$ which corresponds to 10% of total data for each realization. Fig. 14 shows the plots of (frequency × duration) versus duration averaged for 50 different realizations of Markov time series. The error bars are the standard deviations among 50 realizations. The solid curve gives the averaged results for 50 separate realizations. The dashed curve is reproduced from CSM. In none of the 50 cases did any discontinuity appear near seven days. However in four of 50 cases

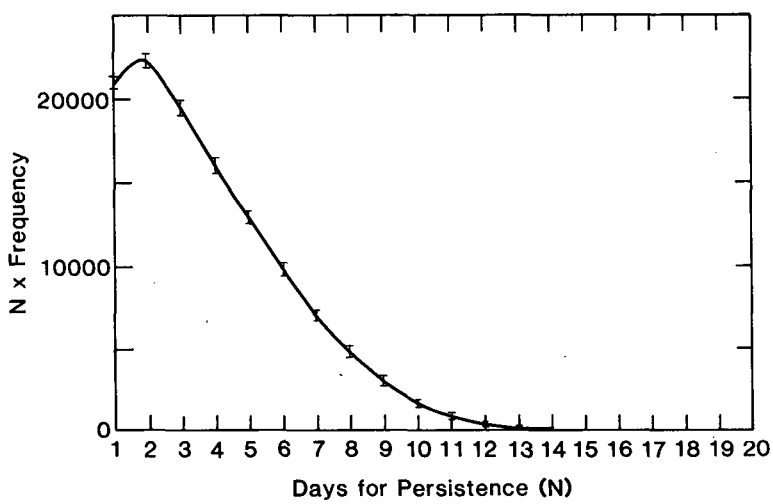

FIG. 15. As in Fig. 14, averaged over 50 sets of a time series with realistic space–time spectra but random phases.

a discontinuity appeared near 11–12 days. It is clear that the sample size is extremely small for 11–12 day persistence.

We also found that if the sample size was reduced from 604 800 to 475 200, a discontinuity occurred at nine days for one case and at 10–11 days for four more cases of 50. If the sample size was further reduced to 302 400, a discontinuity occurred at eight days for four of 50 cases. These results suggest that the secondary discontinuity in CSM might more likely be due to some not yet well understood physical process rather than random sampling of data. It should also be pointed out that the primary peak near 2–3 days noted by CSM due to synoptic-scale travelling disturbances is also nonexistent in Markov time series.

b. Time series with realistic space-time spectra

We generated 50 sets of 15 time series with 90 data points for ten latitudes (34–70°N at 4° interval) in such a way that the amplitude of eastward and westward propagating waves for all frequency (w) and wavenumber (k) was similar to the one given by Straus and Shukla (1981) for space–time spectra of observed geopotential height fluctuations during winter over the Northern Hemisphere. To generate each set of 90-day time series, the initial phase was prescribed randomly. Persistent characteristics were analyzed in the same way as CSM for these idealized time series and the result is given in Fig. 15. Error bars are the standard deviations among 50 realizations. It was found that there was no evidence of a secondary peak or discontinuity in any of the cases. We did however find the first primary peak (near 2–3 days) which corresponds to travelling disturbances.

REFERENCES

Austin, J. F., 1980: The blocking of middle latitude westerly winds by planetary waves. *Quart. J. Roy. Meteor. Soc.*, **106,** 327–350.

Blackmon, M. L., 1976: A climatological spectral study of the 500 mb geopotential height of the Northern Hemisphere. *J. Atmos. Sci.*, **33,** 1607–1623.

Brezowsky, H., H. Flohn and P. Hess, 1951: Some remarks on the climatology of blocking action. *Tellus,* **3,** 191–194.

Charney, J. G., and A. Eliassen, 1949: A numerical method for predicting the perturbations of the middle latitude westerlies. *Tellus,* **1,** 38–54.

——, and J. G. Devore, 1979: Multiple flow equilibria in the atmosphere and blocking. *J. Atmos. Sci.*, **36,** 1205–1216.

——, and D. M. Straus, 1980: Form drag instability, multiple equilibria and propagating planetary waves in baroclinic orographically planetary wave systems. *J. Atmos. Sci.*, **37,** 1157–1176.

——, J. Shukla and K. C. Mo, 1981: Comparison of barotropic blocking theory with observation. *J. Atmos. Sci.*, **38,** 762–779.

Dole, R. M., 1978: The objective representation of blocking patterns. The General Circulation: Theory, Modeling and Observation. NCAR Colloquim Notes: Summer 1978, NCAR/CQ − 6 + 1978 − ASP, 404–426.

——, 1982: Persistent anomalies of the extratropical Northern Hemisphere wintertime circulation. Ph.D. thesis. Massachusetts Institute of Technology, 225 pp.

Elliott, R. D., and T. B. Smith, 1949: A study of the effects of large blocking heights on the general circulation in the Northern Hemisphere westerlies. *J. Meteor.*, **6,** 27–85.

Hoskins, B. J., and D. Karoly, 1981: The steady linear response of a spherical atmosphere to thermal and orographic forcing. *J. Atmos. Sci.*, **38,** 1179–1196.

Kalnay-Rivas, E., and Lee-Or Merkine, 1981: A simple mechanism for blocking. *J. Atmos. Sci.*, **38,** 2077–2091.

McWilliams, J. G., 1980: On application of equivalent modons to atmospheric blocking. *Dyn. Atmos. Oceans.*, **5,** 43–66.

Rex, D. F., 1950a: Blocking action in the middle troposphere and its effects upon regional climate. I. An aerological study of blocking action. *Tellus,* **2,** 196–211.

——, 1950b: Blocking action in the middle troposphere and its effects upon regional climate. II. The climatology of blocking action. *Tellus,* **2,** 275–301.

Straus, S. M., and J. Shukla, 1981: Space–time spectral structure of a GLAS general circulation model and a comparison with observations. *J. Atmos. Sci.*, **38,** 902–917.

Sumner, E. J., 1954: A study of blocking in the Atlantic–European sector of the Northern Hemisphere. *Quart. J. Roy. Meteor. Soc.*, **80,** 402–416.

White, E. B., and N. E. Clark, 1975: On the development of blocking ridge activity over the central North Pacific. *J. Atmos. Sci.*, **32,** 489–501.